



HAL
open science

Coagulation methods and drying step are the key drivers of the dynamics of structuration of natural rubber during the maturation of coagula

Jidapa Noinart, Jérôme Sainte Beuve, Laurent Vaysse, Natedao Musigamart, Françoise Granet, Albert Flori, Siriluck Liengprayoon, Kittipong Rattanaporn, Frederic Bonfils

► To cite this version:

Jidapa Noinart, Jérôme Sainte Beuve, Laurent Vaysse, Natedao Musigamart, Françoise Granet, et al.. Coagulation methods and drying step are the key drivers of the dynamics of structuration of natural rubber during the maturation of coagula. *Express Polymer Letters*, 2022, 16 (11), pp.1161-1176. 10.3144/expresspolymlett.2022.85 . hal-03800236

HAL Id: hal-03800236

<https://hal.inrae.fr/hal-03800236v1>

Submitted on 10 Mar 2023

HAL is a multi-disciplinary open access archive for the deposit and dissemination of scientific research documents, whether they are published or not. The documents may come from teaching and research institutions in France or abroad, or from public or private research centers.

L'archive ouverte pluridisciplinaire **HAL**, est destinée au dépôt et à la diffusion de documents scientifiques de niveau recherche, publiés ou non, émanant des établissements d'enseignement et de recherche français ou étrangers, des laboratoires publics ou privés.



Distributed under a Creative Commons Attribution - NonCommercial - NoDerivatives 4.0 International License

Research article

Coagulation methods and drying step are the key drivers of the dynamics of structuration of natural rubber during the maturation of coagula

Jidapa Noinart^{1,2,3,6}, Laurent Vaysse^{2,3}, Natedao Musigamart¹, Jérôme Sainte-Beuve^{2,3}, Albert Flori^{4,5}, Siriluck Liengprayoon¹, Kittipong Rattanaporn⁶, Françoise Granet⁷, Frederic Bonfils^{2,3*}

¹KAPI, Kasetsart University, 10900 Bangkok, Thailand

²CIRAD, UPR BioWooEB, F-34398 Montpellier, France

³BioWooEB, Univ Montpellier, CIRAD, Montpellier, France

⁴CIRAD, UMR ABSys, F-34398 Montpellier, France

⁵ABSys, Univ Montpellier, CIHEAM-IAMM, CIRAD, INRAE, Institut Agro, Montpellier, France

⁶Department of Biotechnology, Faculty of Agro-Industry, Kasetsart University, 10900 Bangkok, Thailand

⁷Manufacture Française des Pneumatiques MICHELIN, F-63000 Clermont-Ferrand, France

Received 30 March 2022; accepted in revised form 3 July 2022

Abstract. The evolution of the mesostructure (structuring dynamics) of natural rubber (NR) during maturation after different modes of coagulation is poorly known, especially inside wet coagula. Therefore, coagula made from 3 different coagulation modes (sulfuric acid, formic acid, and natural coagulations) with different maturation durations (0, 2, 9, 16, 30, and 44 days) were studied. The mesostructure of NR samples was analyzed using SEC-MALS on wet coagula and on wet and dry crepes. For wet coagula coagulated with acids, only M_z and M_w decreased slightly with maturation time, while M_n and $Gel_{>1\ \mu}$ had no significant evolution during maturation. On the other hand, for wet coagula after natural coagulation, all mesostructure indicators evolved significantly with maturation time. The results showed that structuration increased along maturation time, generating microaggregates with larger size and more structured macrogel inside wet coagula after natural coagulation. This study found that creping process (comparison of wet coagula and wet crepes) had only a moderate effect on the structuration of NR samples. However, the drying process (comparison of wet and dry crepes) had an important effect on the structuration of rubber, especially for natural coagulation and formic acid coagulation. Coagulation with sulfuric acid appeared to slow down the phenomena related to the structuration of microaggregates and macrogel.

Keywords: rubber, latex coagulation, structuration, maturation, SEC-MALS

1. Introduction

1.1. Context and objectives

Natural rubber (NR) produced from *Hevea* trees is an important raw material for several industries, especially for tire manufacturing. Indeed, NR has very specific properties compared to synthetic rubber, such as high resistance to deformation and fracture, low internal heat built-up and high elasticity [1]. Block

rubber, also called technically specified rubber (TSR), such as TSR10 and TSR20 grades, is the main exporting product. These TSR grades are made from field coagula obtained after natural or acid coagulation of field latex [2, 3]. The coagula, after a certain period of storage/maturation, are processed in dry block rubber (Figure 1). From the time that latex exudes from the tree until the end of the industrial

*Corresponding author, e-mail: frederic.bonfils@cirad.fr

© BME-PT

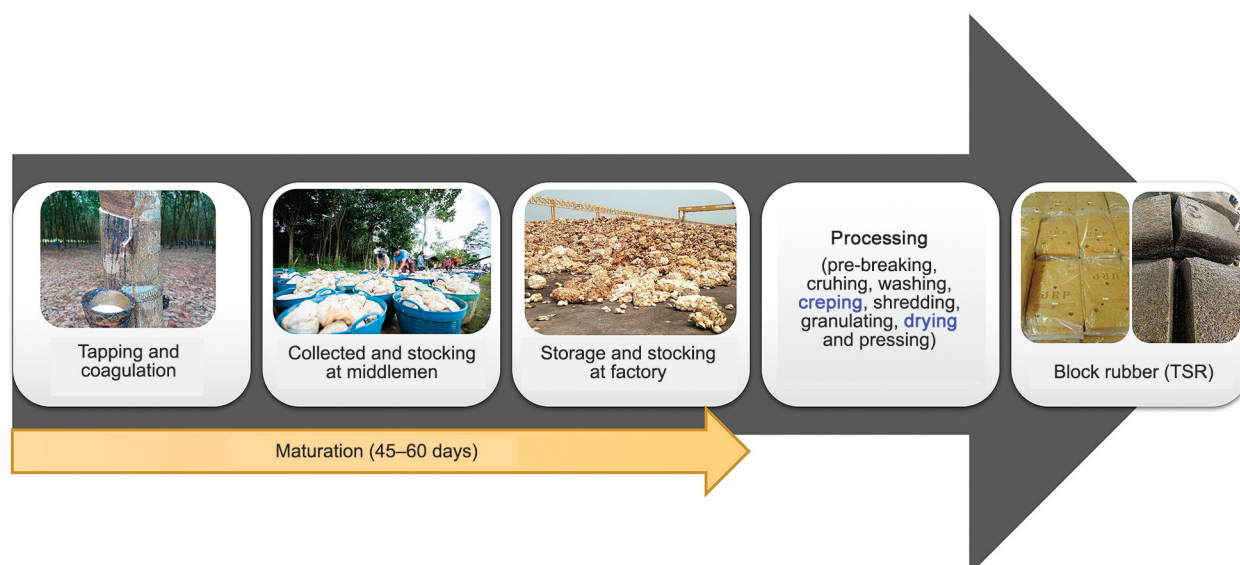


Figure 1. Diagram of block rubber (TSR) processing.

process giving block rubber, little is known on the evolution of the mesostructure of NR (dynamics of structuration). Our main objective was to better know the mesostructure evolution during maturation, especially in wet coagulum. Therefore, we analyzed wet coagulum by size exclusion chromatography coupled to a multi-angular light scattering detector (SEC-MALS) to avoid any modification of mesostructure due to creping/drying. In a second step of the study, we evaluate the influence of creping and drying on the structuration of NR samples.

1.2. The mesostructure of natural rubber

Characterization of NR mesostructure and identification of pertinent criteria allow better understanding and forecasting of the physical properties of NR as other polymers [4–6]. NR differs from its synthetic counterparts in its complex associative or self-assembling structure. After dissolving the NR in a good solvent for the polyisoprene, a variable amount of insoluble material always remains, called the macrogel or gel phase, according to the authors (Figure 2) [7–9]. After removal of the macrogel, usually by centrifugation, the resulting solution contains a mixture of polyisoprene chains (random coil) and compact microaggregates or microgels (sphere-like structure) (Figure 2) [7, 10–13]. For this reason, for natural rubber (NR), as for other biopolymers probably, it is rather simplistic to speak and characterize only the macromolecular structure (soluble polymeric chains). It is important to also quantitatively and qualitatively characterize the aggregates [10, 14–17]. Various disciplines (sociology, linguistics, metallurgy, etc.) use

the notion of macrostructure in order to distinguish the global (large-scale) structure from the local or microstructure (small-scale). For natural rubber, we consider an intermediate scale, the *mesostructure* (structure at the mesoscale) concerning macromolecular structure plus aggregates (Figure 2), which appears to be a good terminological compromise. The notion of mesostructure was met essentially in the field of porous materials science. But, since the beginning of the year 2000, the concept seems to migrate towards the study of multiphase materials, in particular some semi-crystalline copolymers [18]. Today, this notion of the meso-, intermediate level between macro and micro, is more and more used in many disciplines. In an inclusive approach to this topic of structure and structuration of NR, we should also mention the concept of Tanaka [19]: *the naturally occurring network*, and that of Kawahara *et al.* [20]: *the organic-inorganic nanomatrix structure*. To characterize the mesostructure of NR, separative technics coupled to a multi-angular light scattering detector (MALS), especially size exclusion chromatography (SEC) is most probably today the better compromise. SEC-MALS allows determining several parameters linked to the molar mass (M_n , M_w , and M_z) of macromolecules and a size parameter (radius of gyration or R_g) (Figure 2). SEC-MALS, thanks to the refractometer detector (dRI) allow also quantifying the fraction (macrogel plus part of microaggregates, Figure 2) eliminated by filtration before injection. Using a disposable filter of 1 μm porosity, we can determine the quantity of this eliminated fraction called gel superior to 1 μm ($Gel_{>1\mu}$) [4, 7, 19]. Rolere *et al.* [21] showed

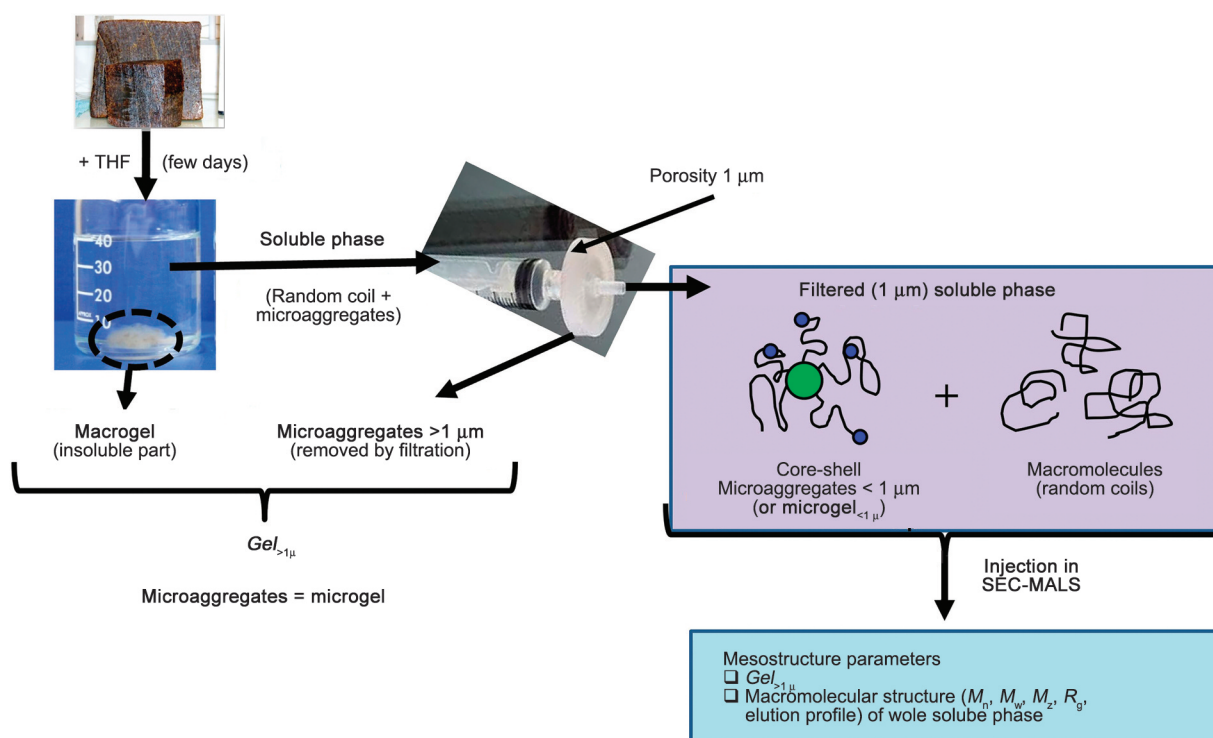


Figure 2. Different types of gels (aggregates) in a solution of natural rubber in tetrahydrofuran (THF) (Figure adapted from Liengprayoon *et al* [7]), and all parameters are given after SEC-MALS analysis. ($Gel_{>1\mu}$: gel superior to 1 μ , M_n : number-average molar mass, M_w : weight-average molar mass, M_z : z-average molar mass, R_g : radius of gyration, I : polymolecularity index).

that the $Gel_{>1\mu}$ offers better NR characterization than macrogel rate in relation to rheological properties.

1.3. The maturation of natural rubber coagula

TSR10 and TSR20 are the main exporting dry rubber products, mostly produced from cup coagula. Cup coagula are latex of rubber trees coagulated by natural coagulation or acid-induced coagulation in the field cups. After coagulation and storage on the plantation for a few days, coagula are transported directly to a factory or accumulated at a middleman premise before being delivered to a factory. Coagula is stocked in a pile at the factory for a period of time (several weeks). The time period starting from tree tapping to coagula processing is called ‘maturation’ (Figure 1). This maturation step is sometimes necessary in order to obtain enough quantity of coagula before processing or even to obtain a required rubber quality with better consistency [22].

The initial Wallace plasticity (P_0) and plasticity retention index (PRI) are important quality indicators of produced TSR. In our previous study [23], we identified and ranked several factors involved during maturation that influence the quality of the obtained block rubber. In this study, which involved two

genotypes (PB235 and RRIM600), it was found that coagulation mode was the most influencing factor of P_0 , PRI, and mesostructure indicators of rubber. Zhong *et al.* [24] showed that acid coagulated rubber had better resistance to thermal oxidation (higher PRI) and lower vulcanization rate than the natural (or spontaneous) coagulated ones. Increasing the natural maturation time (from 2 to 30 days) of coagula gave rubber with lower nitrogen content, higher vulcanization rate, and better mechanical properties (larger maximum torque). Intapun *et al.* [25] reported that a high quantity of microorganisms at the initial stage of maturation enhanced the sensitivity of rubber to thermo-oxidation (decrease in PRI). Concurrently, a higher quantity of microorganisms promoted crosslinking between rubber chains (increase in $Gel_{>1\mu}$) and decreased the weight-average molar mass (M_w) after maturation. Intapun *et al.* [22] showed that storage conditions, including temperature, humidity, the depth within the stocking pile, oxygen content, and the presence of microorganisms, influence P_0 , PRI, and gel content. They found P_0 , PRI, gel content ($Gel_{>1\mu}$), and M_w of NR samples made from matured cup coagula increased significantly with the depth within the coagula pile. Very recently, Chen *et al.* [26] showed that the coagulation method used

(natural, with formic acid, or with salt (CaCl_2)) could influence the mesostructure and properties (P_0 , PRI and green strength) of raw NR. Salomez *et al.* [27] reviewed the strong correlation between the development of microorganisms in latex and rubber coagula during maturation and the evolution of rubber compositions, structure, and properties. For example, microorganisms' concentration increased during the early stage of maturation; their activities affected the production or/and consumption of fatty acids and other organic acids and the degradation of sugars and proteins. The microbial communities present in natural rubber coagula during maturation were characterized and identified by Salomez *et al.* [28]. They found that after two days of maturation, the main microorganisms were composed of lactic acid bacteria (LAB) in anaerobic conditions, while Actinobacteria was the dominant microbial group in aerobic conditions. Indeed, lipase and esterase activities of *Pseudoclavibacter*, a genus of Actinobacteria class, lead to the release of free fatty acids with pro-oxidant properties, leading to rubber chain scissions. Recently, Guan *et al.* [29] studied the influence of added sugar in latex before natural coagulation (2 days) on nitrogen and mineral element contents, the structuration of NR and NR properties. They proposed that the network architecture of raw NR can be adjusted by glucose loading by varying the content and existing state of polyisoprene chain terminals and metal ions in the network.

To monitor and study the influence of maturation conditions on NR properties and mesostructure, we developed an experimental pilot who can control the maturation conditions as described in Noinart *et al.* [23]. In this study, the latex was coagulated in a newly developed maturation chamber, which can control/ monitor many conditions during the maturation of coagula, including temperatures, relative humidity, coagulation modes, clones, vertical forces, and maturation durations. After maturation, coagula were passed through creping and drying processes. Each sample was analyzed by SEC-MALS as wet coagulum, wet crepe, and dry crepe to determine the dynamics of evolution of the mesostructural criteria of each type of sample (wet coagulum, wet crepe, and dry crepe). These results also allowed the evaluation of the impact of the transformation processes (creping and drying) on the natural rubber structuring.

2. Materials and methods

2.1. Source of natural rubber and raw material preparation

Rubber samples were made from the latex of *Hevea brasiliensis* trees from the plantation of Visahakit Thai Rubber Co., Ltd. located in Chantaburi province, Thailand. RRIM600 clone was chosen because it is by far the most planted clone in Thailand. Three groups of 70–80 RRIM600 trees were selected as the source of 3 repetitions. The trees were stimulated with 0.8 g of ethephon (2.5%) on a tree's panel every 30–45 days (about 8 times/year). The selected trees were tapped during the night (about 1–2 am). The tapping system was S/2, d3 (the trees are tapped on one half spiral cut tapped downward 1 day out of 3 days). In the morning (about 5–7 am), latex was collected in the field cups about 4–5 hours after tapping. The latex was filtrated through a stainless sieve (pore size, 1.0 mm). The collected latex (around 9 l per repetition) was poured and gently mixed in 10 l jerrycans (one per repetition) and disposed in an ice box for transportation.

Once back in the laboratory, latex was poured into the corresponding empty cups (200 ml/cup). There were three coagulation modes (natural coagulation, formic acid coagulation, and sulfuric acid coagulation). We selected these 2 acidic modes of coagulation because they are used by farmers in Thailand for fast coagulation in the cup. Coagulation was either natural or induced by addition of 10 ml of 5% formic acid or 5% sulfuric acid and gentle stirred by hand with a glass rod for around 20 seconds. In case of unmaturation coagula samples (day 0 of maturation), only the samples treated by acid coagulation could be made. They were processed (creping, drying) around 1 h after acid addition. For the other days of maturation, all coagula of latex were stored in the plastic cups placed in the controlled maturation device at 45 °C, 70% RH and O_2 providing by air pump for 2 days in order to complete coagulation especially the coagula that treated with natural coagulation. After 2 days, all plastic cups were removed and coagula were returned back into the maturation device. The experiment was operated for 44 days (including 2 days of coagulation) to cover maturation durations (2, 9, 16, 30 and, 44 days) that are representative of the real industrial period. Mesostructure were measured on 3 coagula from each combination (Figure 3).

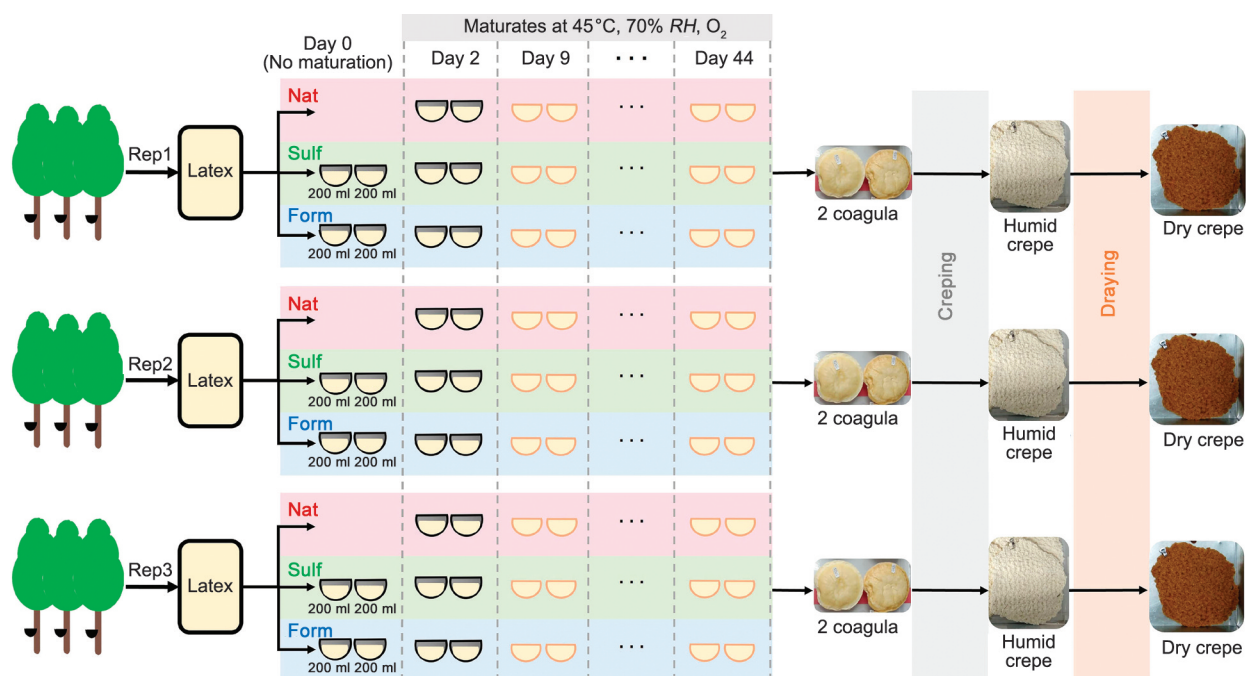


Figure 3. Maturation steps and coagula processing.

For the purpose of mesostructure analysis, 2–3 g of coagula were sampled before processing by creping and drying. To obtain the dry rubber, each sampled coagula was creped with 2 single passes, 12 double passes, and 3 single passes using a water flow rate of 10 l/min to obtain a 10 mm (± 2 mm) thick crepe. The creper machine was supplied by TSP (1010 SERIES, Bangkok, Thailand) and had the following specifications: roll diameter 250 mm, roll length 500 mm, diamond type groove, space between grooves 4 mm, groove depth 4 mm, groove width 4 mm, gap between rolls less than 1 mm, and roll speeds 17 rpm (front) and 15 rpm (rear), hence friction of 1.13. The obtained crepes were dried in a hot-air oven (OF-155, 1.6 kW, DAIHAN Scientific Co., Ltd., Korea) at 115 °C for 3 h, cooled in a desiccator, and weighed. Dry crepes were cut for 2–3 g before homogenizing step. The homogenized method used in this study followed SMR Bulletin No.7, Part B.2, 1992 standard. After homogenizing step, all homogenized crepes were cut 2–3 g for further tests. All types of 2–3 g samples were kept in a freezer (-20°C) before analysis by SEC-MALS.

2.2. Sample preparation for mesostructure analysis by SEC-MALS

In order to obtain a sample concentration of about 1 mg/ml, 30 \pm 3 mg of sample (coagulum or wet crepe or dry crepe) were dissolved in 30 ml of HPLC grade tetrahydrofuran (THF, Fisher, Montpellier, France)

stabilized with 2,6-di-*tert*-butyl-4-methylphenol (BHT, Fisher, Montpellier, France) at 250 mg/l. The solvent (stabilized THF) was filtrated at 0.1 μm before use. All sample solutions were stored at 30 °C in the dark in a water bath for 1 week with daily stirred by hand. After 7 days, the rubber solution was filtrated (Acrodisc 1 μm , glass fiber, Pall, Paris, France) to remove the macrogels and part of the microgels. After filtration, samples were injected into a size exclusion chromatography coupled to a multi-angle light scattering detector and a refractometer (SEC-MALS).

2.3. SEC-MALS analysis

SEC-MALS chromatography line consists of a refractometer (dRI) (Wyatt Optilab rEX, Wyatt, Toulouse, France, at 658 nm and 30 °C), a Wyatt multi-angle light scattering detector at 633 nm (Dawn HELEOS II, Wyatt, Toulouse, France,) and a SHIMADZU HPLC line (DGU-20A3R degasser, LC20AD pump, CTO-20A column oven, SIL20AHT injector, Montpellier, France). The columns, maintained at 45 °C, are two PL gel mixed (Varian, 20 μm , 300 mm \times 7.5 mm I.D., Montpellier, France) with a guard column. The mobile phase is THF stabilized with BHT at a flow rate of 0.65 ml/min. The injected volume is 100 μl . All diode detectors at all 18 angles in the MALS detector were normalized using a THF solution of low polydisperse polystyrene standard ($M_w = 34$ kg/mol, Polymer Standards Service). The

same solution was used to determine the interconnection volume between the two detectors (0.175 ml). Number-average molar mass (M_n), weight-average molar mass (M_w) and z-average molar mass (M_z) were calculated using ASTRA software version 6.1.7.16 (Wyatt technology). The order of polynomial fit used with the Berry method is two. All light scattering angles and dRI baselines were adjusted for the calculation. The differential refractive index increment (dn/dc) value at 633 nm depends on the pair of sample and solvent; it is 0.130 ml/g for NR in THF [30]. ASTRA software (Wyatt, Toulouse, France) performed all the calculation from the chromatogram by integrating the whole peak corresponding to polyisoprene on the chromatogram. Apart from the average molar masses and radius of gyration, ASTRA software allows knowing the quantity of matter eluted through the columns, and so the exact quantity of matter injected (m_1), thanks to the dRI detector. For that, the surface of the polyisoprene peak is integrated by ASTRA software. Thus, the amount of matter that passes through the filter is known (m_1). As we know exactly the concentration of the solution before filtration and the injected volume (0.1 ml), we can calculate the initial amount of matter before filtration (m_0). The fraction eliminated by filtration is called the gel superior to 1 μm ($Gel_{>1\mu}$) and can be calculated with Equation (1):

$$Gel_{>1\mu} [\%] = \frac{m_0 - m_1}{m_0} \cdot 100 \quad (1)$$

An approximation is made by considering that all the material passed through the 1 μm filter and injected in SEC-MALS is found in the polyisoprene peak. It is not excluded that some material remains trapped in the columns. It should also be kept in mind that this gel is slightly overestimated because it is not corrected for non-isoprene compounds passing through the filter and eluting after the polyisoprene peak. This systematic error can be estimated at about 2%.

2.4. Statistical data treatment

All statistical treatments were done with JMP software (SAS, Paris, France).

Hypothesis is tested by an ANOVA including the interactions between the creping or drying status of the sample and the 2-order orthogonal polynomials of the maturation time.

3. Results and discussion

3.1. Mesostructure evolved inside wet coagula during maturation at a different place depending on the coagulation method used (acidic or natural)

To better know the mesostructure evolution along with maturation, we analyzed by SEC-MALS wet coagula samples to avoid modification of mesostructure due to creping/drying. Samples were analyzed after 0, 2, 9, 16, 30 and 44 days of maturation. Figure 4 presents the evolution of the determined mesostructure indicators: the number-average molar mass (M_n), the weight-average molar mass (M_w), the z-average molar mass (M_z) and the gel superior to 1 μm ($Gel_{>1\mu}$) along with maturation after the 3 different types of coagulation. After sulfuric or formic acid coagulation (Figure 4a and 4b), only M_z and M_w evolved significantly with time. M_z and M_w decreased with maturation time, while no significant evolution was observed for M_n and $Gel_{>1\mu}$. For sulfuric coagulation, M_z decreased from 2760 to 1800 kg/mol and M_w from 1420 to 1090 kg/mol during maturation. After formic coagulation (Figure 4b), M_z decreased from 2530 to 1800 kg/mol and M_w from 1310 to 1040 kg/mol. For sulfuric coagulation, if we compare the samples after 2 and 44 days of maturation (Figure 5), we can see that the elution profiles remained bimodal after 44 days of maturation. The main significant difference was in the molar masses (M_i) profile at the beginning of elution. After 44 days, the M_i profile is lower compared to the one for 2 days of maturation (see a blue circle in Figure 5). The elution time (t_e) is proportional to the elution volume (V_e) of the column set. The elution volume is proportional to the hydrodynamic radius (R_h) of the eluting macromolecule. In other words, macromolecules eluting at the same t_e have the same hydrodynamic volume. For the same elution time (or elution volume, or hydrodynamic volume), higher M_i was observed for 2 days maturation compared to 44 days maturation. This implies that denser entities (more compact) elute at the beginning of the chromatogram for coagula after only 2 days of maturation. This phenomenon explains the lower M_z observed after 44 days of maturation compared to 2 days of maturation. It can be assumed that a lower quantity of microaggregates (sphere-like structure) eluted with long-chain polyisoprene (random coil structure) in the case of 44 days compared to 2 days.

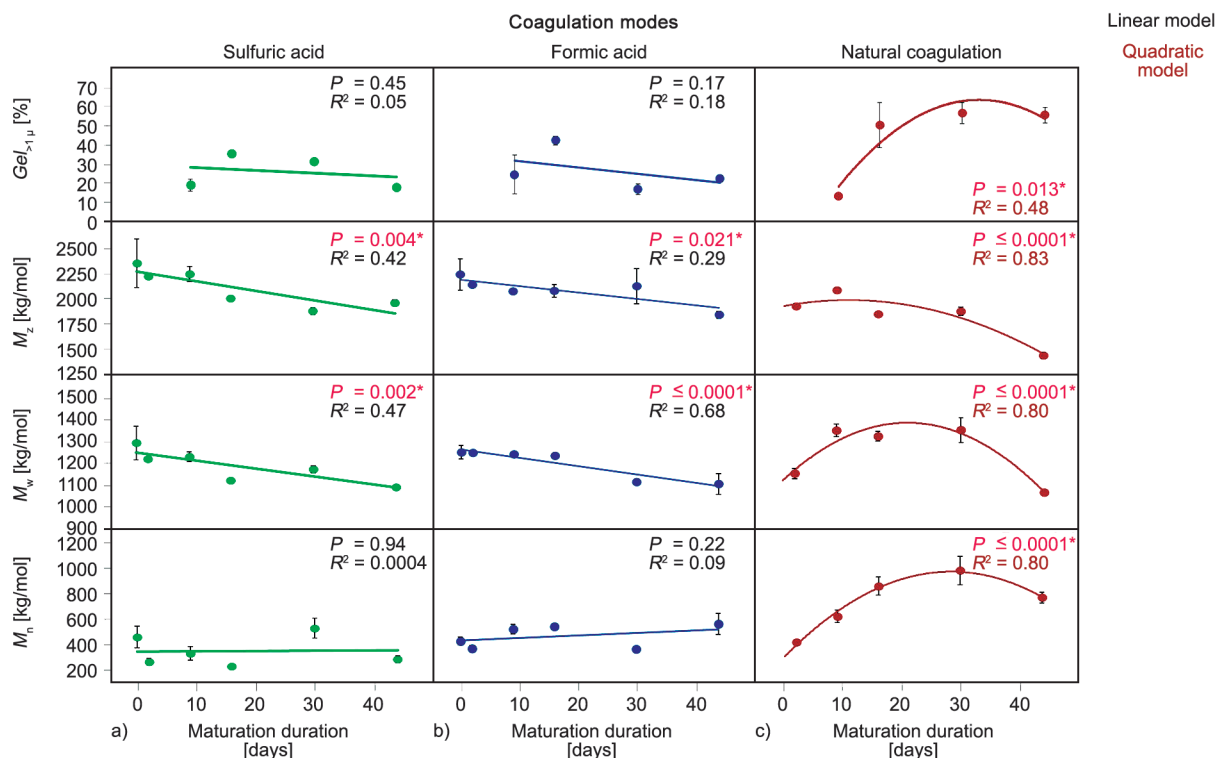


Figure 4. Mesostructure (M_n , M_w , M_z , $Gel_{>1 \mu}$) evolution of wet coagula during maturation after (a) coagulation with sulfuric acid (green) (b) coagulation with formic acid (blue) and (c) natural coagulation (no acid, red). * of P value means a significant difference with maturation time.

The same phenomenon was observed for samples after formic acid coagulation (data not shown). These results for acid coagulation let us think there is no significant scission of long polyisoprene chain due to microorganism’s activity during maturation of coagula as proposed by Salomez *et al.* [28] for natural coagulation.

For natural coagulation, all parameters of mesostructure evolved significantly with maturation duration

(Figure 4c). However, these evolutions with maturation duration do not follow a linear model but are better fitted with a quadratic model (M_w and M_n) or appeared occurring in two stages ($Gel_{>1 \mu}$ and M_z). After natural coagulation, M_n and M_w of samples increased significantly with maturation time until a maximal value at about 30 days of maturation and decreased for longer maturation duration. Unlike M_n and M_w , M_z stayed constant until 30 days of maturation and decreased afterward. On the contrary, $Gel_{>1 \mu}$ increased at the beginning of the maturation and remained constant afterward. It can be noticed that after natural coagulation $Gel_{>1 \mu}$, M_n and M_w reached significantly higher values than those of acid-induced coagulations. Unlike the 2 acid coagulations, if we look at the elution profile and the molar mass profile (Figure 6), we can notice huge changes between short and long maturation times. The bimodal elution profile for 2 day maturation became unimodal after 44 days of maturation. It can also be noticed that after 44 days of maturation, part of the long chains (red hatched zone on the left of Figure 6) is no more present. Most probably, these long chains exhibited scissions, thanks to special microorganisms as proposed by Salomez *et al.*, [27]. The maturation

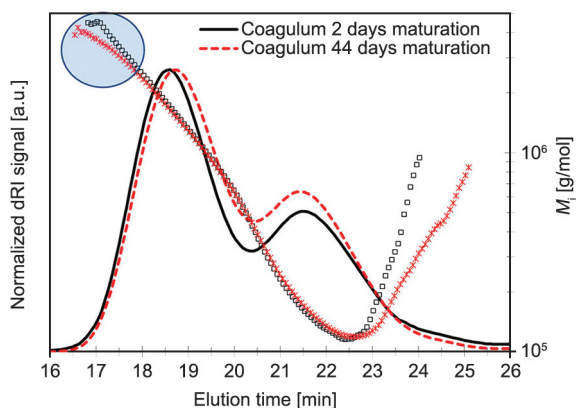


Figure 5. Chromatogram showing the refractometer signal (dRI), or elution profile, and molar mass (M_i) profiles for coagula coagulated by sulfuric acid coagulation from maturation day 2 (black) and day 44 (red).

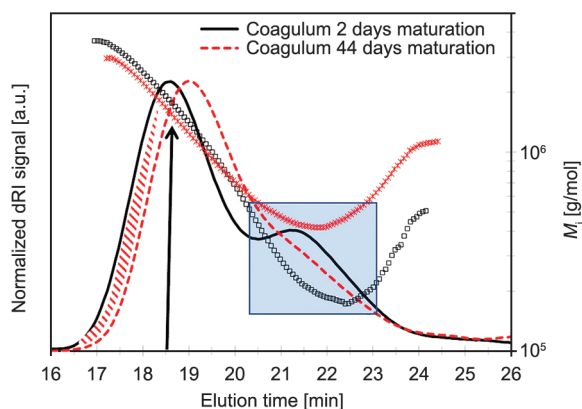


Figure 6. Chromatogram showing the refractometer signal (dRI), or elution profile, and molar mass (M_i) profiles for coagula after natural coagulation from maturation day 2 (black) and day 44 (red).

of the coagula was done at 45 °C, so it can be thought oxidation took place due to this quite high temperature during maturation. However, for acid coagulation, though this high temperature, no significant chain scission was noticed. Therefore, it can be assumed that scissions of long polyisoprene chains for natural coagulation are due to the presence of special microorganisms [27]. The molar mass (M_i) profile also significantly changed with a huge abnormal elution for 44 days of maturation compared to 2 day maturation (see blue square in Figure 6). As shown by Kim *et al.* [12], this abnormal elution profile is due to the co-elution of microaggregates with short chains (low M_i). It can also be noticed that at the beginning of elution (see black arrow in Figure 6), for the same elution time, the M_i is higher for 2 day maturation compared to 44 days of maturation. As proposed previously for sulfuric coagulation, this phenomenon can be due to less microaggregates eluting with long polyisoprene chains at the beginning of the chromatogram for 44 days of maturation. We can think that these microaggregates reacted together along maturation to form higher size microaggregates and so an increase of abnormal elution, as observed (blue square in Figure 6) and also an increase of macrogel quantity as seen in Figure 7. Indeed, after 44 days of maturation we can definitively see a big piece of macrogel (Figure 7b). After 2 days of maturation, only small pieces of macrogel could be seen (Figure 7a). We can also see in Figure 7 that the THF solution obtained after 2 days of maturation is cloudy, while the one obtained after 44 days of maturation is clear. Taken together, these results show that under the maturation conditions used, significant changes in

mesostructure occur inside wet coagula obtained by natural coagulation. The addition of sulfuric acid for latex coagulation largely inhibits this dynamic of structuration. We can assume that the low latex pH obtained with sulfuric acid ($1 < \text{pH} < 2$) will slow down or even inhibit the enzymatic activities (endogenous and exogenous) in the medium and probably disturb the development of microorganisms. This hypothesis would agree with the work of Intapun *et al.* [25], who showed that increasing the amount of microorganisms in the latex leads to an increase in $Gel_{>1 \mu}$.

3.2. Creping has a very low impact on mesostructure whatever the coagulation mode

To study the effect of creping on mesostructure along maturation time, SEC-MALS data (M_n , M_w , M_z , $Gel_{>1 \mu}$) from wet coagula and wet crepes were compared (Figure 8), for the 3 different coagulation modes (sulfuric, formic, and natural). All samples were analyzed after 0, 2, 9, 16, 30 and 44 days of maturation. Whatever the coagulation mode and the mesostructure indicators, we can observe the same trends of evolution during maturation duration for wet coagula and wet crepes. As an example, the decrease of M_z with maturation time observed previously for wet coagula was also observed for wet crepes (Figure 8). It can be observed for some mesostructure indicators, especially M_n and M_w , lower values for wet crepe compared to wet coagula (the difference being materialized by the red zone). In order to assess whether these differences are significant (or not), we used the statistical method described in the experimental section. All calculated probabilities after ANOVA are summarized in Table 1. Thus, significant differences between wet coagula (blue line) and wet crepes (green dash line) were obtained for M_n and M_w of samples, whatever the coagulation mode (red arrow in Figure 8). M_z of sulfuric coagulated samples also appeared significantly different after creping ($P = 0.012$, Table 1). The main impact of creping is to reduce the M_n and M_w of samples slightly whatever the coagulation modes.

3.3. Drying is an essential factor in the structuration of natural rubber

Figure 9 presents the evolution of mesostructure parameters (M_n , M_w , M_z and $Gel_{>1 \mu}$) along with maturation for wet crepes (before drying, green dash line)

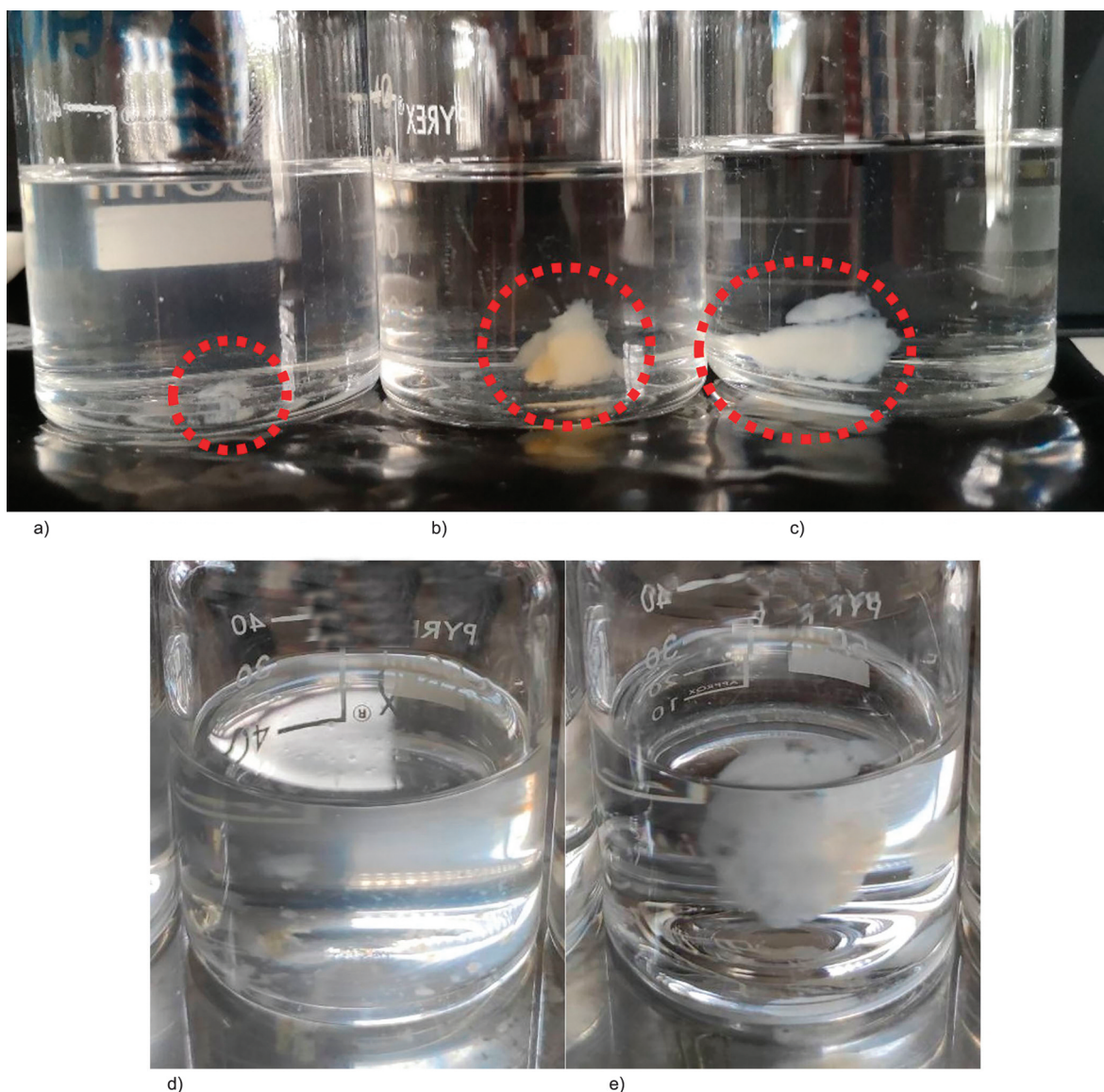


Figure 7. Samples after 7 days in solution in tetrahydrofuran: (a) wet coagulum after 2 days maturation, (b) wet coagulum after 44 days maturation, (c) dry crepe after 2 days maturation. Red dotted circle allows focus on macrogel and visual observation of macrogel in the rubber solutions of wet crepes (d) and dry crepes (e) obtained from samples treated by natural coagulation after 44 days of maturation.

and dry crepes (after drying, purple dotted line) for the 3 different modes of coagulation. We can observe the same trends of evolution along with maturation duration for wet crepes and dry crepes, except for M_n of natural coagulated samples. Though M_n increased with maturation time for wet crepes, M_n decreased with maturation time for the dry crepe. We can see that drying had a very significant influence on many mesostructure indicators (Table 2, yellow area on Figure 9). Except $Gel_{>1\mu}$ for sulfuric coagulation and M_w for formic coagulation, all other indicators evolved more or less significant because of drying (yellow area in Figure 9, Table 2). The most affected samples are those after natural coagulation and the ones coagulated with formic acid. For crepes

produced from latex coagulated by sulfuric acid, drying influenced only M_z ($P < 0.0001$, Table 2) and M_n ($P = 0.0001$, Table 2) significantly. Drying resulted in a slight decrease of M_z (about 16%), and an increase of M_n (about 38%), especially for maturation duration equal to or above 9 days. For samples from formic coagulation, M_z decreased highly significantly while M_n and $Gel_{>1\mu}$ increased highly significantly after drying (yellow area on Figure 9b, Table 2). For M_z , the significant difference between the 2 slopes for the linear model ($P = 0.038$, Table 2) shows that the difference of M_z between wet and dry crepe increased significantly with maturation time (Figure 9b).

To better understand these evolutions linked to drying, it is necessary to analyze in detail the obtained

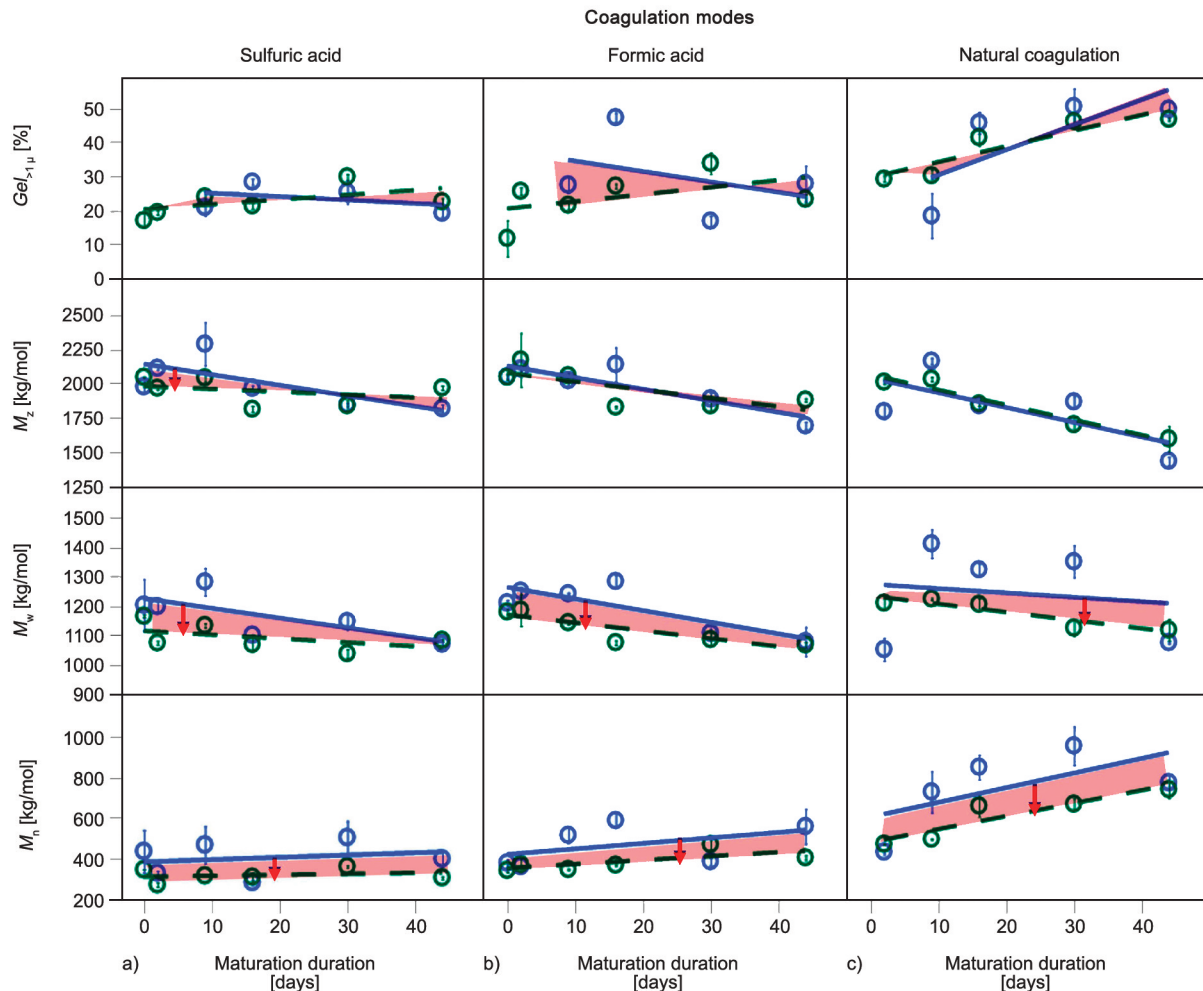


Figure 8. Mesostructure (M_n , M_w , M_z , $Gel_{>1 \mu}$) of wet coagula (blue line), wet crepes (green dash line) by coagulation modes – (a) sulfuric acid; (b) formic acid; (c) natural coagulation – during 44 days of maturation; the red area is the effect of creping. All graphs with a red arrow mean a significant influence of creping was determined (Table 1).

Table 1. Statistical data were obtained to evaluate the creping effect (wet coagula models versus wet crepe models) (if $P < 0.05$, red values → significant differences).

	Tested hypothesis	Sulfuric coagulation	Formic coagulation	Natural coagulation
$Gel_{>1 \mu}$	different constant (Mean)	$P = 0.3300$	$P = 0.8500$	$P = 0.2000$
	different slope (Linear trend)	$P = 0.9200$	$P = 0.7000$	$P = 0.0060$
	different curvature (Quadratic model)	$P = 0.2500$	$P = 0.4700$	$P = 0.0250$
M_z	different constant (Mean)	$P = 0.0119$	$P = 0.4500$	$P = 0.8400$
	different slope (Linear trend)	$P = 0.0036$	$P = 0.2300$	$P = 0.3700$
	different curvature (Quadratic model)	$P = 0.5500$	$P = 0.1500$	$P = 0.0050$
M_w	different constant (Mean)	$P = 0.0001$	$P = 0.0005$	$P = 0.0023$
	different slope (Linear trend)	$P = 0.0176$	$P = 0.1800$	$P = 0.7800$
	different curvature (Quadratic model)	$P = 0.8000$	$P = 0.0530$	$P = 0.0007$
M_n	different constant (Mean)	$P = 0.0036$	$P = 0.0142$	$P = 0.0001$
	different slope (Linear trend)	$P = 0.6600$	$P = 0.0100$	$P = 0.9400$
	different curvature (Quadratic model)	$P = 0.4900$	$P = 0.9200$	$P = 0.0023$

elution profiles (dRI signal) and M_i profiles ($M_i = f(t_e)$). Figure 10 gives the elution profiles and the M_i profiles after maturation at day 2, 9, 30 and 44, comparing wet and dry crepes for samples coagulated

with formic acid. Several changes can be observed in Figure 10. Firstly, the bimodal elution profiles (dRI signal) of wet crepes became unimodal under the action of drying, except for 2 days of maturation,

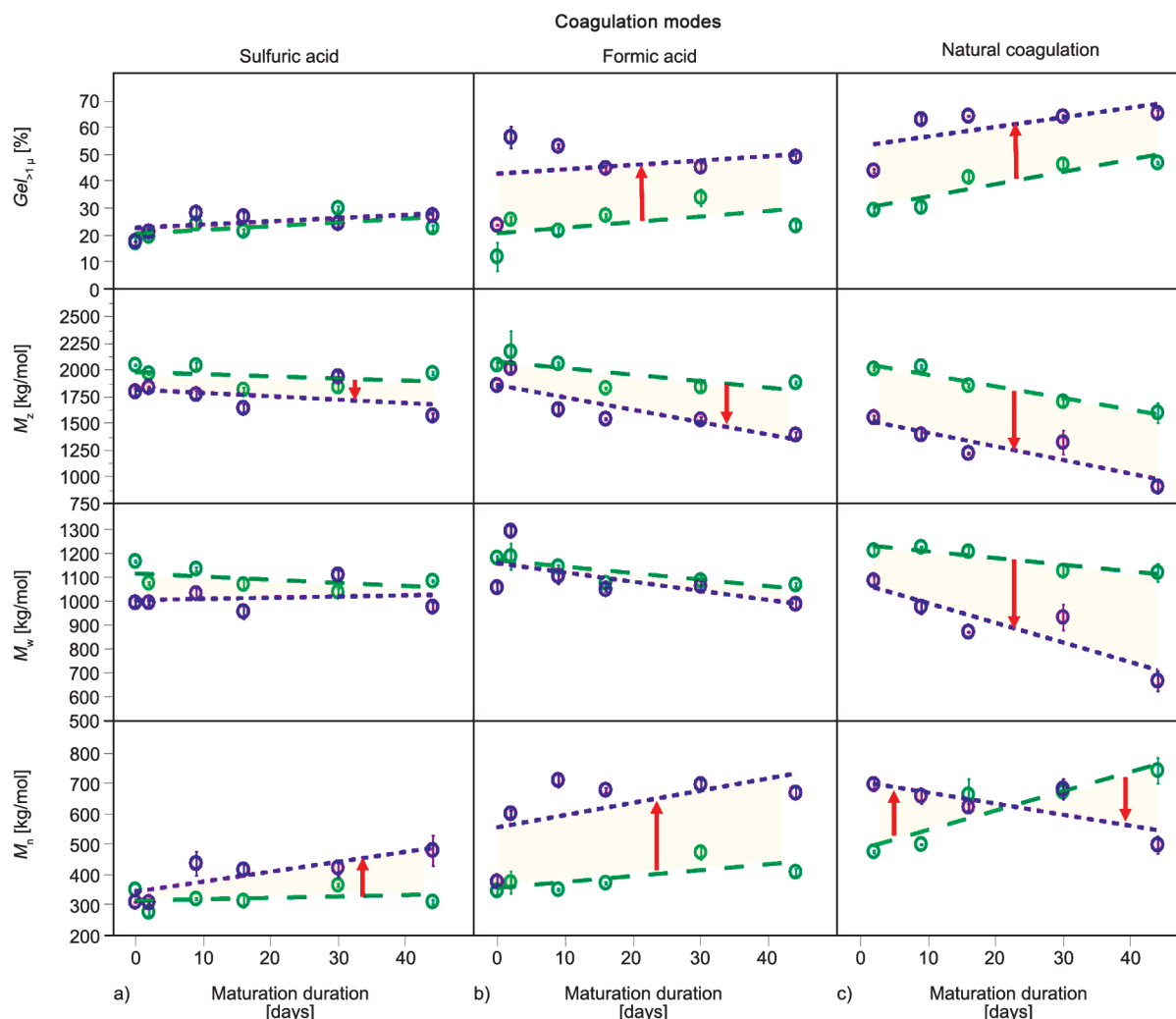


Figure 9. Mesostructure (M_n , M_w , M_z , $Gel_{>1 \mu}$) of wet crepes (green dash line) and dry crepes (purple dot line) by coagulation modes – (a) sulfuric acid; (b) formic acid; (c) natural coagulation – during 44 days of maturation; the yellow area is the effect of drying. All graphs with a red arrow mean a significant influence of drying was determined (Table 2).

Table 2. Statistical data obtained to evaluate the drying effect (dry crepe models versus wet crepe models) (red values → significant differences).

	Tested hypothesis	Sulfuric coagulation	Formic coagulation	Natural coagulation
$Gel_{>1 \mu}$	different constant (Mean)	$P = 0.1900$	$P < 0.0001$	$P < 0.0001$
	different slope (Linear model)	$P = 0.9400$	$P = 0.7700$	$P = 0.4000$
	different slope (Curve model)	$P = 0.6600$	$P = 0.4800$	$P = 0.2250$
M_z	different constant (Mean)	$P < 0.0001$	$P < 0.0001$	$P < 0.0001$
	different slope (Linear model)	$P = 0.8200$	$P = 0.0380$	$P = 0.5100$
	different slope (Curve model)	$P = 0.0140$	$P = 0.9100$	$P = 0.5700$
M_w	different constant (Mean)	$P = 0.0930$	$P = 0.1500$	$P < 0.0001$
	different slope (Linear model)	$P = 0.0420$	$P = 0.4200$	$P = 0.0100$
	different slope (Curve model)	$P = 0.8000$	$P = 0.5100$	$P = 0.7500$
M_n	different Constant (Mean)	$P = 0.0001$	$P < 0.0001$	$P = 0.4300$
	different slope (Linear model)	$P = 0.0085$	$P = 0.1800$	$P < 0.0001$
	different slope (Curve model)	$P = 0.5200$	$P = 0.0300$	$P = 0.9900$

when the dried sample remained bimodal. It can also be noticed a small shift of the dRI signal in the zone of long chains (lower t_c , red arrows). This phenomenon

can be due to chain scissions of longer polyisoprene chains because of thermo-oxidation during drying. Secondly, we can see an increase in the abnormal

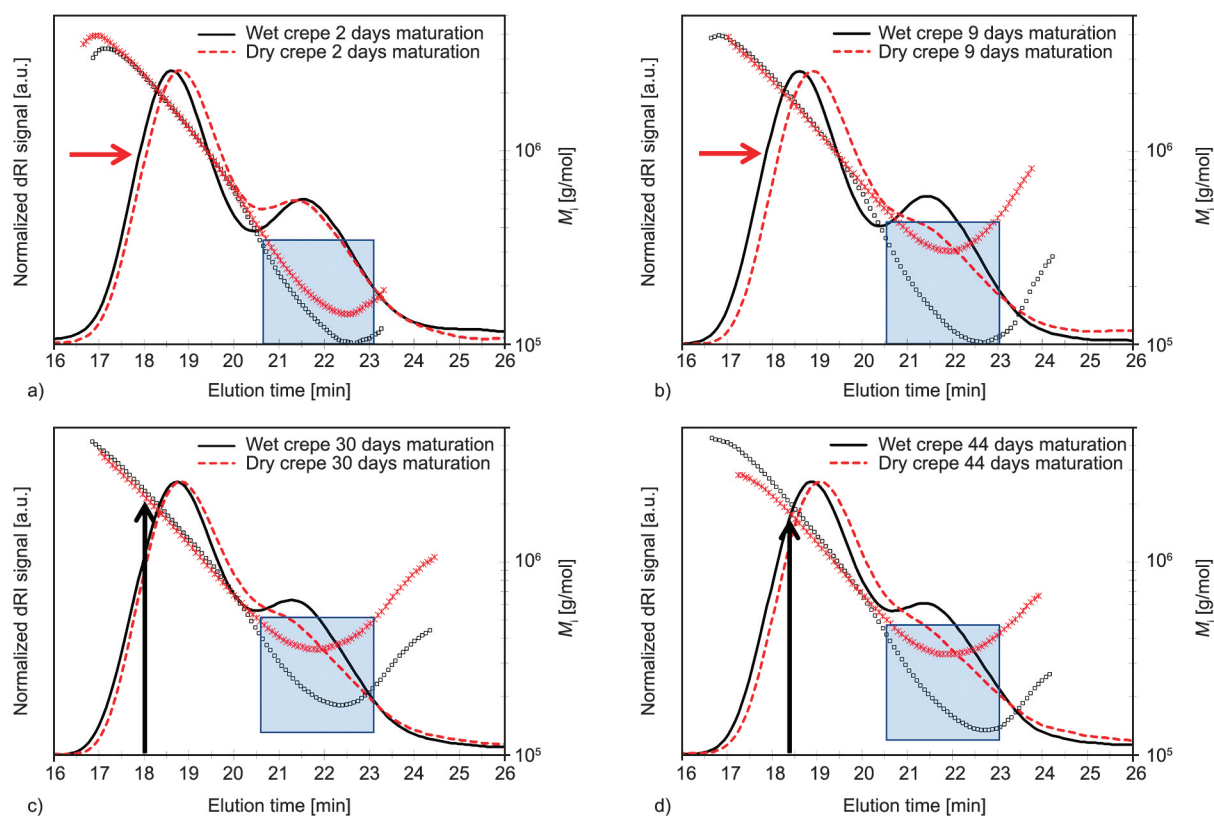


Figure 10. Chromatogram showing the refractometer signals (dRI), or elution profiles, and molar mass (M_i) profiles for humid and dry crepes after coagulation with formic acid: (a) 2 days of maturation, (b) 9 days of maturation, (c) 30 days of maturation and (d) 44 days of maturation.

elution in the short polyisoprene chain zone (blue squares, Figure 10). As previously explained, this abnormal elution profile is due to the co-elution of microaggregates with short polyisoprene chains (low M_i). Thirdly, the M_i at the beginning of the elution (zone of long polyisoprene chains, black arrows, Figure 10c and 10d) for dry crepes appeared lower than the ones for wet crepes of maturation day 9, 30 and especially day 44. This phenomenon can also explain the lower M_z obtained for dry crepes compared to wet crepes. This phenomenon was also observed comparing wet coagula after 2 and 44 days of natural maturation (Figure 6). For Figure 10, smaller M_i for the same elution time (t_e) suggests that the polyisoprene chains are denser (more compact) for wet crepes. It is likely that at the shortest t_e (long-chain area), a mixture of random coil and microaggregates elutes, more or less rich in microaggregates depending on the type of sample. This was confirmed by the conformation plot ($R_{gi} = f(M_i)$), Figure 11). For crepes obtained with coagula matured 44 days, the blue circle in Figure 11b shows smaller R_{gi} for the same M_i in the case of wet crepe versus dry crepe, so denser entities for wet crepes. For crepes

obtained with coagula matured 2 days (D2), no significant difference appeared on the conformation plot between wet and dry crepes (Figure 11a). For the extreme case, after 44 days of natural maturation (Figure 11c), the difference between the conformation plots between wet and dry crepe is even more important. For the wet crepe, the slope for the linear part of $R_{gi} = f(M_i)$ (Flory exponent) is 0.53 but 0.61 for the dry crepe. Knowing the theoretical value of the Flory exponent is 0.59 for a random coil, macromolecules eluting for the dry crepe is closer to random coil conformation than those eluting for the wet crepe. These results show that the phenomenon already observed by comparing coagula after 2 and 44 days (D44) of maturation (Figure 6), *i.e.* structuring of microaggregates, is exacerbated by drying. These results suggest that the microaggregates present at D2 gradually aggregate together to form larger microaggregates that were more delayed during elution and eluting with short chains increasing the abnormality of M_i elution (see the blue square in Figure 10). These data with the increase of $Gel_{>1\mu}$ rate (Figure 9) with drying let us think drying led to an essential structuration of coagulated samples.

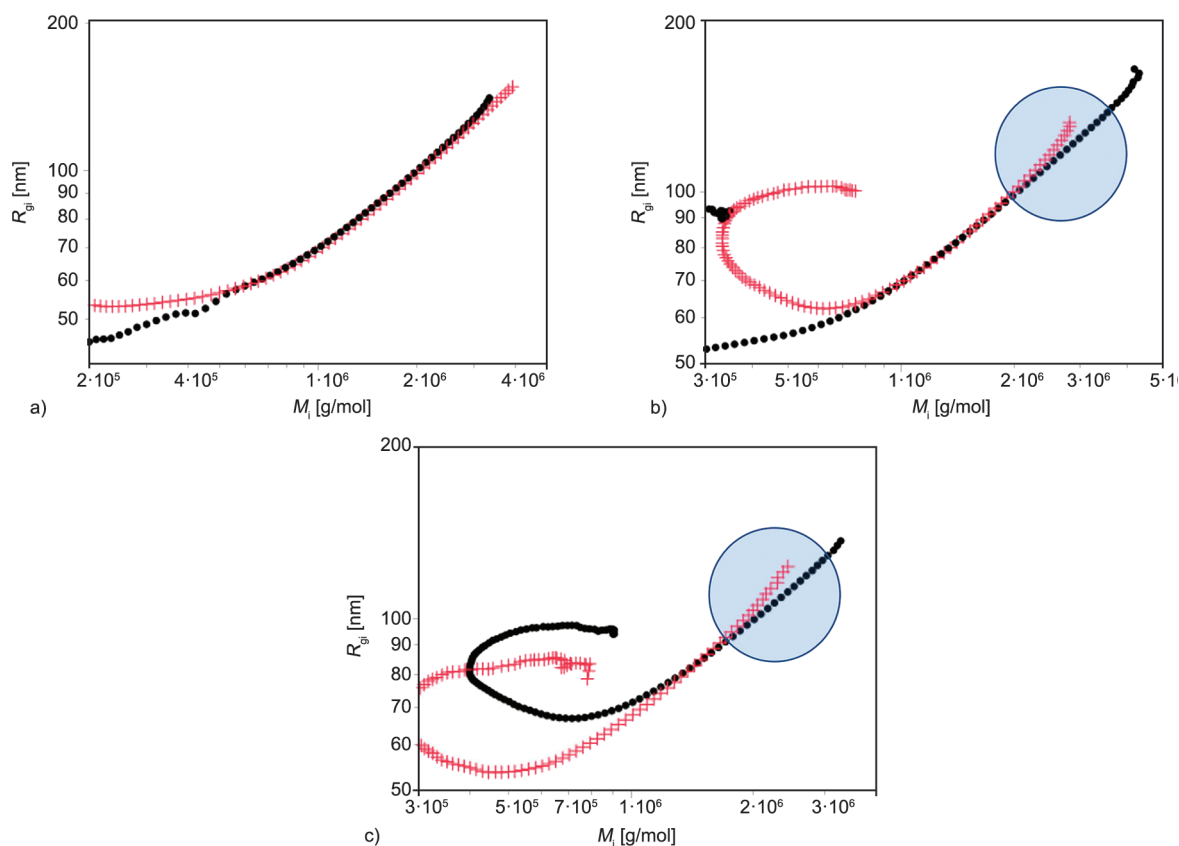


Figure 11. Log-log plots of R_{gi} versus M_i (conformation plot) for wet crepe (black) and dry crepe (red) after formic acid coagulation for (a) 2 days of maturation and (b) 44 days of maturation, (c) after 44 days of natural coagulation.

Elimination of water by drying could favor contact and/or reactivity of microaggregates to form larger ones and even macrogel (Figure 7e). We can assume that reactions between abnormal groups on polyisoprene chains (aldehyde [31] and/or esters [19] and/or proteins [19, 32]) are promoted during drying. We can see in Figure 7d that macrogel is less structured, and the solution is still cloudy for wet crepe than for dry crepe.

Overall, the changes in the elution profiles (dRI signal and M_i) for samples coagulated with formic acid are also visible for samples coagulated naturally or with sulfuric acid (Figures 12 and 13). However, these changes are more or less pronounced depending on the type of coagulation (natural or sulfuric). Samples coagulated by sulfuric acid (Figure 12) exhibited the least changes on elution profiles (dRI signal) and M_i profiles and the ones coagulated by natural coagulation (Figure 13) showed the most important changes, following data presented in Figure 9. After 2 days of maturation (D2), Figure 13a for natural coagulation clearly shows that the abnormal elution is higher than for formic acid coagulation (Figure 10). Furthermore, after 2 days of maturation,

for natural coagulation (Figure 13a), we also clearly see a difference in the M_i profiles that were not observed for crepes from coagula coagulated with formic acid (Figure 10). These results show that sulfuric acid slows down the phenomena behind the structuration of microaggregates. On the other hand, for natural coagulation, structuration appears to be faster than for coagulation with formic acid.

4. Conclusions

For the first time, the evolution of NR mesostructure was studied in wet coagula along with maturation duration after three modes of latex coagulation: i) natural coagulation, ii) with formic acid, or iii) with sulfuric acid. The results from this study showed that mesostructure evolved inside wet coagula along with maturation at different paces, depending on the coagulation method used (acid-induced or natural). After acid coagulation, the changes of the mesostructure in the coagula are minimal (only a slight decrease of M_w and M_z , elution profiles remained bimodal) but much more pronounced for the natural coagulation. After natural coagulation $Gel_{>1 \mu}$, M_n and M_w reached significantly higher values than

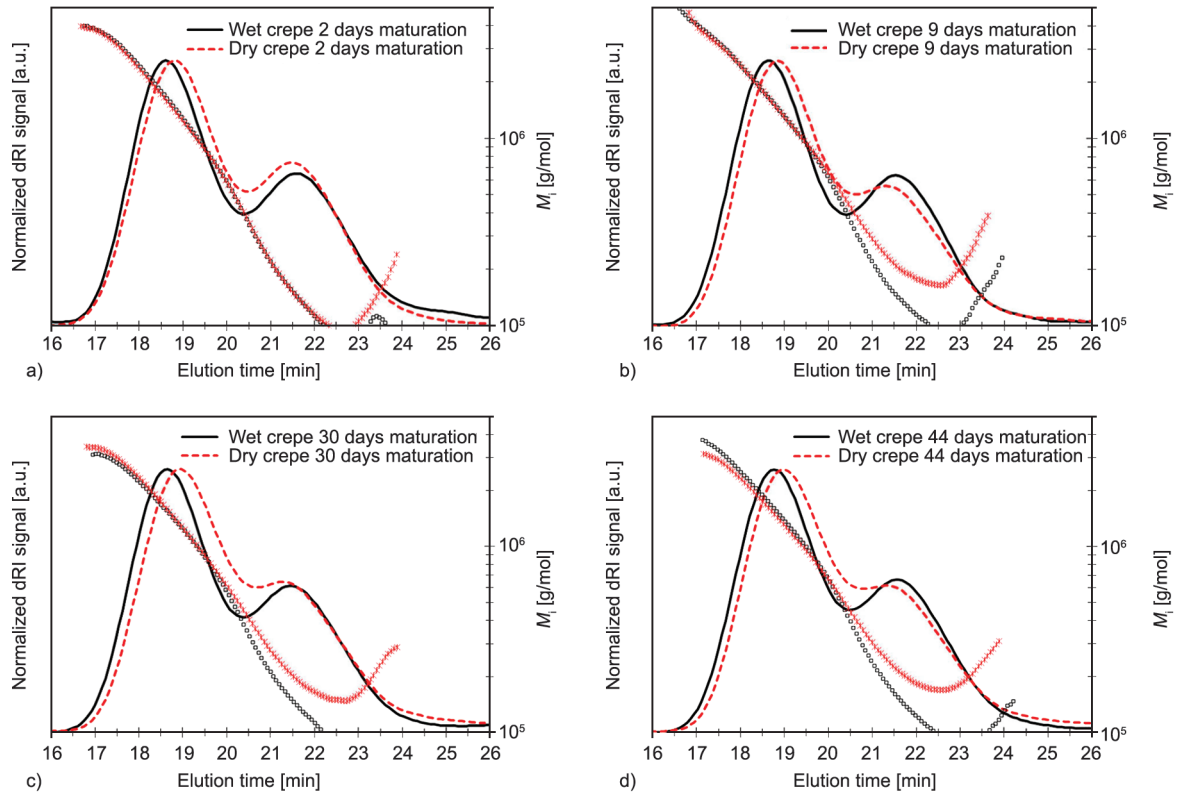


Figure 12. Chromatogram showing the refractometer signal (dRI), or elution profile, and molar mass (M_i) profiles for wet crepe (black) and dry crepe (red) after sulfuric acid coagulation for maturation day 2 (a), day 9 (b), day 16 (c) and day 44 (d).

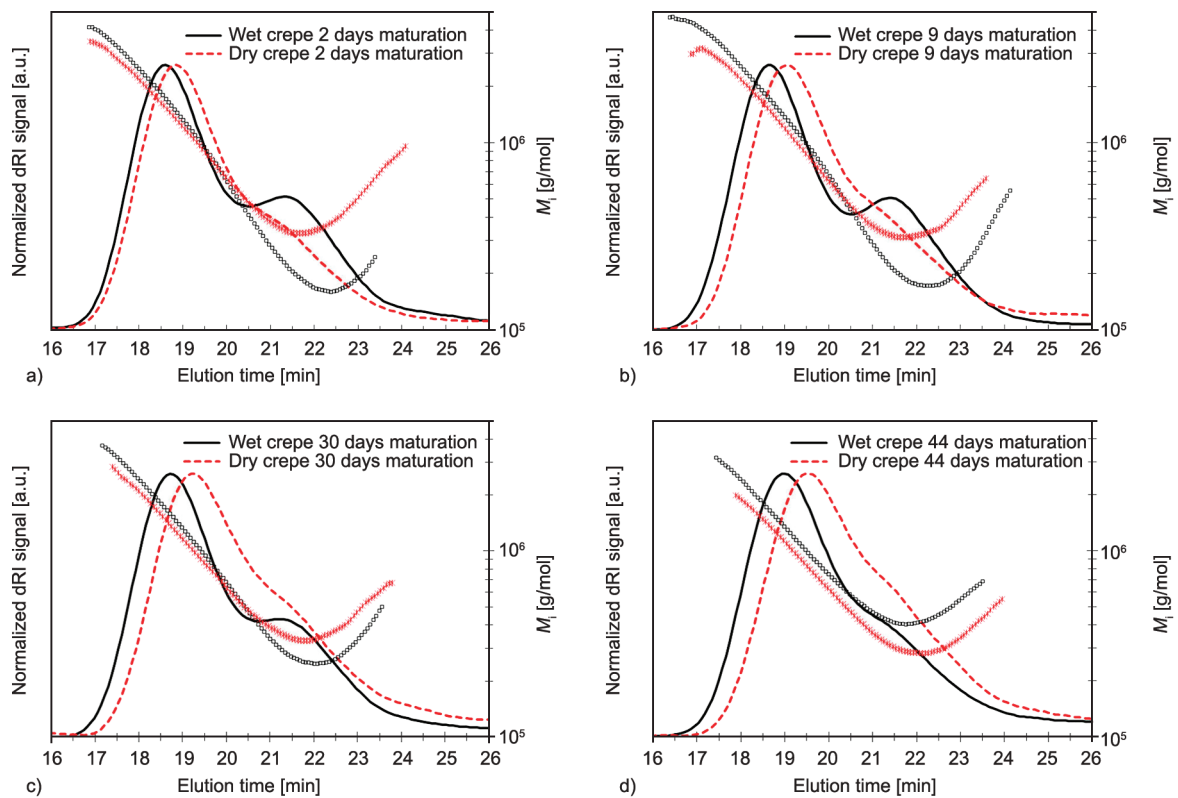


Figure 13. Chromatogram showing the refractometer signal (dRI), or elution profile, and molar mass (M_i) profiles for wet crepe (black) and dry crepe (red) after natural coagulation for maturation day 2 (a), day 9 (b), day 16 (c) and day 44 (d).

those of acid-induced coagulation with important modifications to the elution profiles (bimodal became unimodal) and the molar mass profiles along maturation time. The results let us think a progressive structuration took place inside the coagula, along with maturation, with a change in microaggregates sizes and a higher macrogel structuration.

Comparing mesostructure indicators for wet coagula to those for wet crepes showed that creping had a very low impact on mesostructure. Only M_w and M_n evolved significantly with creping. M_w and M_n slightly decreased under the action of creping, whatever the coagulation mode used.

Finally, we compared the mesostructure indicators obtained for dry crepes to those of wet crepes. The drying strongly influenced the NR structuring. Here also, we observed a progressive structuring of the NR, more important as the maturation time increases. We observed an evolution of the microaggregate structuration and a pronounced evolution of the elution profiles (bimodal became unimodal) during the maturation and according to the conditions used for the coagulation (natural, formic acid or sulfuric acid). These results show that acid coagulation, especially sulfuric one, slows down the phenomena related to the NR structuration compared to natural coagulation. We suppose that the aggregation is limited because of a slowing down, more or less pronounced according to the acid used, of the enzymatic activities in the medium and very probably of the development of the microorganisms.

These results show that depending on the coagulation conditions used by the farmers, the mesostructure of the humid coagula and the NR blocks resulting from these coagula can vary greatly. It is therefore highly likely that the properties (quality) of the block rubber will also vary greatly.

Acknowledgements

The authors thank Manufacture Française des Pneumatiques Michelin, France, for financial support and thank Visahakit Thai Rubber Co., Ltd for kindly providing latex from their plantation. This work was undertaken under the framework of the Hevea Research Platform in Partnership (HRPP), Thailand.

References

[1] Mark J. E., Erman B., Roland M.: The science and technology of rubber. Academic Press, Boston (2013).

[2] George P., Jacob C. K.: Natural rubber agromanagement and crop processing. Rubber Research Institute of India, Kerala (2000).

[3] Wisunthorn Pansook S., Chambon B., Sainte-Beuve J., Vaysse L.: Natural rubber quality starts at the smallholdings: Farmers' cup coagulum production in southern Thailand. *Journal of Rubber Research*, **18**, 87–98 (2015).

[4] Roberts A. D.: Natural rubber science and technology. Oxford University Press, Oxford (1988).

[5] Ferry J. D.: Viscoelastic properties of polymers. Wiley, New York (1980).

[6] Ehabé E., Bonfils F., Aymard C., Akinlabi A. K., Sainte Beuve J.: Modelling of mooney viscosity relaxation in natural rubber. *Polymer Testing*, **24**, 620–627 (2005). <https://doi.org/10.1016/j.polymertesting.2005.03.006>

[7] Liengprayoon S., Chelbi K., Dubascoux S., Char C., Vaysse L., Dubreucq E., Sainte Beuve J., Sriroth K., Bonfils F.: Mesostructure characterization by asymmetrical flow field-flow fractionation of natural rubber samples from different *Hevea brasiliensis* genotypes. *Industrial Crops and Products*, **109**, 936–43 (2017). <https://doi.org/10.1016/j.indcrop.2017.09.062>

[8] Tanaka Y., Tarachiwin L.: Recent advances in structural characterization of natural rubber. *Rubber Chemistry and Technology*, **82**, 283–314 (2009). <https://doi.org/10.5254/1.3548250>

[9] Wisunthorn S., Liengprayoon S., Vaysse L., Beuve J. S., Bonfils F.: SEC-MALS study of dynamic structuring of natural rubber: Comparative study of two *Hevea brasiliensis* genotypes. *Journal of Applied Polymer Science*, **124**, 1570–1577 (2012). <https://doi.org/10.1002/app.35099>

[10] Dubascoux S., Thepchalerm C., Dubreucq E., Wisunthorn S., Vaysse L., Kiatkamjornwong S., Nakason C., Bonfils F.: Comparative study of the mesostructure of natural and synthetic polyisoprene by size exclusion chromatography-multi-angle light scattering and asymmetrical flow field flow fractionation-multi-angle light scattering. *Journal of Chromatography A*, **1224**, 27–34 (2012). <https://doi.org/10.1016/j.chroma.2011.12.010>

[11] Kim C., Morel M-H., Sainte Beuve J., Guilbert S., Collet A., Bonfils F.: Characterization of natural rubber using size-exclusion chromatography with online multi-angle light scattering: Study of the phenomenon behind the abnormal elution profile. *Journal of Chromatography A*, **1213**, 181–188 (2008). <https://doi.org/10.1016/j.chroma.2008.10.052>

[12] Kim C., Sainte Beuve J., Guilbert S., Bonfils F.: Study of chain branching in natural rubber using size-exclusion chromatography coupled with a multi-angle light scattering detector (SEC-MALS). *European Polymer Journal*, **45**, 2249–2259 (2009). <https://doi.org/10.1016/j.eurpolymj.2009.05.015>

- [13] Rolere S., Bottier C., Vaysse L., Sainte-Beuve J., Bonfils F.: Characterisation of macrogel composition from industrial natural rubber samples: Influence of proteins on the macrogel crosslink density. *Express Polymer Letters*, **10**, 408–419 (2016).
<https://doi.org/10.3144/expresspolymlett.2016.38>
- [14] Bonfils F., Doumbia A., Char C., Beuve J. S.: Evolution in the natural rubber native structure and plasticity retention index from the first tapping of clonal trees. *Journal of applied polymer science*, **97**, 903–909 (2005).
<https://doi.org/10.1002/app.21845>
- [15] Rippel M. M., Leite C. A., Lee L-T., Galembeck F.: Direct imaging and elemental mapping of microgels in natural rubber particles. *Colloid and Polymer Science*, **283**, 570–574 (2005).
<https://doi.org/10.1007/S00396-004-1187-Z>
- [16] Shiibashi T.: Gel structure characterization of NR and IR and direct observation of individual polymer molecules by electron microscopy. *International Polymer Science and Technology*, **14**, T33–T39 (1987).
- [17] Rolere S., Cazevieille C., Sainte-Beuve J., Bonfils F.: New insights on natural rubber microgel structure thanks to a new method for microaggregates extraction. *European Polymer Journal*, **80**, 117–125 (2016).
<https://doi.org/10.1016/j.eurpolymj.2016.05.008>
- [18] Jouenne S., González-León J. A., Ruzette A-V., Lodefier P., Tence-Girault S., Leibler L.: Styrene/butadiene gradient block copolymers: Molecular and mesoscopic structures. *Macromolecules*, **40**, 2432–2442 (2007).
<https://doi.org/10.1021/ma062723u>
- [19] Tanaka Y.: Structural characterization of natural polyisoprenes: Solve the mystery of natural rubber based on structural study. *Rubber Chemistry and Technology*, **74**, 355–375 (2001).
<https://doi.org/10.5254/1.3547643>
- [20] Kawahara S., Yusof N. H., Noguchi K., Kosugi K., Yamamoto Y.: Organic–inorganic nanomatrix structure and properties of related naturally occurring rubbery macromolecules. *Polymer*, **55**, 5024–5027 (2014).
<https://doi.org/10.1016/j.polymer.2014.07.026>
- [21] Rolere S., Cartault M., Sainte-Beuve J., Bonfils F.: A rheological method exploiting cole-cole plot allows gel quantification in natural rubber. *Polymer Testing*, **61**, 378–385 (2017).
<https://doi.org/10.1016/j.polymertesting.2017.05.043>
- [22] Intapun J., Sainte-Beuve J., Bonfils F., Tanrattanakul V., Dubreucq E., Vaysse L.: Characterisation of natural rubber cup coagula maturation conditions and consequences on dry rubber properties. *Journal of Rubber Research*, **12**, 171–184 (2009).
- [23] Noinart J., Bonfils F., Musigamart N., Sainte-Beuve J., Flori A., Liengprayoon S., Rattanaporn K., Granet F., Vaysse L.: Post-harvest maturation of *Hevea brasiliensis* latex coagula: Ranking of the key drivers of the mesostructure and physical properties of natural rubber. *Journal of Rubber Research*, **25**, 5–18 (2022).
<https://doi.org/10.1007/s42464-022-00146-7>
- [24] Zhong J-P., Li C-P., Li S-D., Kong L-X., Yang L., Liao S-Q., She X-D.: Study on the properties of natural rubber during maturation. *Journal of Polymer Materials*, **26**, 351–360 (2009).
- [25] Intapun J., Sainte-Beuve J., Bonfils F., Tanrattanakul V., Dubreucq E., Vaysse L.: Effect of microorganisms during the initial coagulum maturation of *Hevea* natural rubber. *Journal of Applied Polymer Science*, **118**, 1341–1348 (2010).
<https://doi.org/10.1002/app.32331>
- [26] Chen X., Zhang H-F., Zhang L., Wei Y-C., Hu B., Luo M-C., Liao S.: Insight on natural rubber’s relationship with coagulation methods and some of its properties during storage. *Journal of Rubber Research*, **24**, 555–562 (2021).
<https://doi.org/10.1007/s42464-021-00139-y>
- [27] Salomez M., Subileau M., Intapun J., Bonfils F., Sainte-Beuve J., Vaysse L., Dubreucq E.: Micro-organisms in latex and natural rubber coagula of *Hevea brasiliensis* and their impact on rubber composition, structure and properties. *Journal of Applied Microbiology*, **117**, 921–929 (2014).
<https://doi.org/10.1111/jam.12556>
- [28] Salomez M., Subileau M., Vallaeyts T., Santoni S., Bonfils F., Sainte-Beuve J., Intapun J., Granet F., Vaysse L., Dubreucq É.: Microbial communities in natural rubber coagula during maturation: Impacts on technological properties of dry natural rubber. *Journal of Applied Microbiology*, **124**, 444–456 (2018).
<https://doi.org/10.1111/jam.13661>
- [29] Guan J., Zhao F., Gu T., Liu H., Luo M-C., Liao S.: Role of endogenous glucose on natural rubber molecular chains and natural network architecture based on biological action and chelation. *Polymer*, **202**, 122752 (2020).
<https://doi.org/10.1016/j.polymer.2020.122752>
- [30] Kim C., Deratani A., Bonfils F.: Determination of the refractive index increment of natural and synthetic poly(cis-1,4-isoprene) solutions and its effect on structural parameters. *Journal of Liquid Chromatography and Related Technologies*, **33**, 37–45 (2009).
<https://doi.org/10.1080/10826070903427072>
- [31] Sekhar B.: Inhibition of hardening in natural rubber. *Rubber Chemistry and Technology*, **35**, 889–895 (1962).
<https://doi.org/10.5254/1.3539981>
- [32] Grechanovskii V., Dmitrieva I., Zaitsev N.: Separation and preliminary characterisation of the protein component from commercial varieties of *Hevea* rubber. *International Polymer Science and Technology*, **14**, T1–T4 (1987).